



Cite this: DOI: 10.1039/d6ea00023a

Optimizing Vocus proton-transfer-reaction mass spectrometry for detecting trace atmospheric amines

Yiqi Zhao,^a Zhaojin An,^{*a} Yuyang Li,^a Rujing Yin,^b Dandan Li,^a Dongbin Wang,^a Xuan Zheng,^c Jun Zheng,^d Hong He,^e Jincal Zhao,^f Kebin He,^a Douglas R. Worsnop^{ij} and Jingkun Jiang^g^{*a}

Amines, as important alkaline gases in the atmosphere besides ammonia, profoundly influence air quality, climate and human health through various atmospheric processes. Besides well-studied alkylamines, emerging amines (e.g., monoethanolamine (MEA), piperazine (PZ), 2-amino-2-methyl-1-propanol (AMP)) from the rapidly expanding amine-based carbon capture facilities may be emitted into the atmosphere, posing new demands for their measurement. Vocus Proton-Transfer-Reaction Mass Spectrometry (Vocus-PTR) is an effective technique for detecting volatile organic compounds (VOCs), but its capability to measure a broader variety of trace-level amines remains to be explored. In this study, we optimized the focusing ion-molecule reactor condition of Vocus-PTR to improve the chemical ionization efficiency and ion transmission efficiency of amine detection. The optimized Vocus-PTR achieved good performance for detecting both atmospheric amines and VOCs, with limits of detection (LODs) for amines (0.16–0.55 pptv) lower than those for VOCs (9.34–38.79 pptv). The observed shift in the reduced electric field strength (from ~147 to 107–117 Td) indicates an increased abundance of water–cluster reagent ions in the reactor, enhancing the sensitivity and selectivity for amine detection. The optimized instrument was deployed in urban Beijing. C_{2–6}-alkylamines, C_{1–6}-amides and several emerging amines were identified and quantified, showing characteristic diurnal variations.

Received 9th February 2026
Accepted 11th April 2026

DOI: 10.1039/d6ea00023a

rsc.li/esatmospheres

Environmental significance

Atmospheric amines, as key organic alkaline gases, significantly influence air quality, climate, and human health. The amine escape of rapidly expanding carbon capture facilities poses new demands for atmospheric amine measurement. In this study, the focusing ion-molecule reactor condition of Vocus Proton-Transfer-Reaction Mass Spectrometry (Vocus-PTR) were optimized to improve the chemical ionization efficiency and ion transmission efficiency of amine detection, achieving good performance for detecting both atmospheric amines and volatile organic compounds. Using the optimized instrument, several alkylamines, alkylamides and emerging amines were identified and quantified in urban Beijing, showing characteristic diurnal variations. These advancements would facilitate a better understanding of the behavior and evolution of amines in the atmosphere.

1 Introduction

Amines, as the key alkaline gases in the atmosphere besides ammonia, significantly affect air quality, climate and human

health. They facilitate new particle formation and contribute to secondary particulate matter *via* nucleation and heterogeneous reactions.^{1–12} These newly formed particles can further grow into cloud condensation nuclei to affect climate.^{13–17}

^aState Key Joint Laboratory of Regional Environment and Sustainability, School of Environment, Tsinghua University, Beijing, 100084, China. E-mail: jiangjk@tsinghua.edu.cn; azj@tsinghua.edu.cn

^bKey Laboratory of Industrial Ecology and Environmental Engineering (Ministry of Education), School of Environmental Science and Technology, Dalian University of Technology, Dalian, 116024, China

^cCollege of Chemistry and Environmental Engineering, Shenzhen University, Shenzhen, 518060, China

^dNUIST Reading Academy, Nanjing University of Information Science & Technology, Nanjing, 210044, China

^eState Key Joint Laboratory of Environment Simulation and Pollution Control, Research Center for Eco-Environmental Sciences, Chinese Academy of Sciences, Beijing, 100085, China

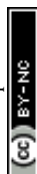
^fUniversity of Chinese Academy of Sciences, Beijing, 100049, China

^gCenter for Excellence in Regional Atmospheric Environment, Institute of Urban Environment, Chinese Academy of Sciences, Xiamen, 361021, China

^hKey Laboratory of Photochemistry, CAS Research/Education Center for Excellence in Molecular Sciences, Institute of Chemistry, Chinese Academy of Sciences, Beijing, 100190, China

ⁱInstitute for Atmospheric and Earth System Research/Physics, Faculty of Science, University of Helsinki, Helsinki 00014, Finland

^jAerodyne Research, Inc., Billerica, Massachusetts 01821, USA



Additionally, their oxidation products (*e.g.*, nitrosamines) pose risks to human health.^{6–9,17} Typical atmospheric alkylamines originate from large-scale natural and anthropogenic sources, such as oceanic and forest emissions, livestock farming, industrial activities, sewage release, and vehicle exhaust.¹⁷ The growing deployment of amine-based carbon capture facilities in recent years raises concerns about new emission sources.^{18–21} Amine absorbents such as monoethanolamine (MEA), piperazine (PZ), and 2-amino-2-methyl-1-propanol (AMP) may potentially emerge and accumulate in the atmosphere, with measured concentrations in flue gas ranging from several to a hundred ppm.^{22–32} Measuring atmospheric amines is thus essential for understanding their composition, abundance, sources, and impacts. Previous studies have conducted field measurements across urban, rural, industrial, coastal, forest and mountainous areas, with the concentrations of atmospheric alkylamines generally falling in the range of 10^{-1} – 10^2 pptv.^{33–60}

Several offline techniques have been developed for measuring atmospheric amines at the early stage. These methods combining offline sampling and laboratory analysis *via* various chromatography methods (gas chromatography, liquid chromatography and ion chromatography) were applied to detect short-chain alkylamines such as dimethylamine (DMA) and trimethylamine (TMA).^{33–45}

Over the past two decades, online techniques for measuring atmospheric amines have been advanced by chemical ionization mass spectrometry (CIMS) (Table S1).^{46–60} Proton-Transfer-Reaction Mass Spectrometry (PTR-MS), using H_3O^+ as the reagent ion, is capable of detecting amines as well as volatile organic compounds (VOCs) since their proton affinity is higher than that of H_2O .^{46–51} It was first reported by Sellegri *et al.*⁴⁷ and Hanson *et al.*,⁴⁶ achieving the online measurements of atmospheric amines. Other systems using protonated water clusters,^{52–54} protonated ethanol^{55–57} and protonated acetone⁵⁸ as reagent ions offer higher selectivity for amine detection due to their closer proton affinity to amines.

Vocus proton-transfer-reaction time-of-flight mass spectrometry (Vocus-PTR) is an improved PTR-MS with enhanced sensitivity and mass resolution for VOC detection, showing potential for simultaneous detection of atmospheric amines.⁶¹ Several studies have demonstrated the performance of Vocus-PTR for amine measurement.^{49,50} Wang *et al.* utilized it to measure atmospheric C_2 -amines in Wangdu, China.⁴⁹ Chang *et al.* deployed it for mobile measurements of DMA and TMA.⁵⁰ However, the capability of Vocus-PTR to measure a broader variety of trace-level amines remains to be demonstrated. Further improvements in performance of Vocus-PTR are needed for trace-level amine detection.

Improving both chemical ionization efficiency and ion transmission efficiency may further improve the detection capability of Vocus-PTR for amines. For the former, increasing the proportion of protonated water clusters in reagent ions improves chemical ionization efficiency, thereby achieving both a higher sensitivity and a better selectivity for amine detection.⁵² Water clusters have a higher proton affinity than H_2O , allowing them to exclude many VOCs with lower proton affinity and thereby enhance detection selectivity for high-proton-affinity amines. Regarding ion transmission efficiency, Wang *et al.*⁴⁹ investigated that big segmented

quadrupole (BSQ) radio frequency (RF) amplitude field modulates DMA transmission *via* mass discrimination; lower voltage enhances transmission efficiency and thus sensitivity.⁶² In addition, the RF field within the focusing ion-molecular reactor (FIMR) region also affects the ion transmission.^{61,63}

In this study, we optimized the FIMR condition of Vocus-PTR for amine detection, orienting towards increasing both chemical ionization efficiency and ion transmission efficiency. The detection performance of the optimized instrument toward amines and VOCs was evaluated. The optimization patterns and their corresponding effects were presented and discussed. Finally, the optimized Vocus-PTR was applied to field measurement of atmospheric amines in urban Beijing during the summer of 2024, and their concentration levels and temporal variations were investigated.

2 Materials and methods

2.1 Instrument and optimization

The main structure of Vocus-PTR (Toferwerk AG and Aerodyne Research Inc., Vocus-2R PTR-TOF-MS) consists of a reagent-ion source, a FIMR, a BSQ, ion lens, and a long time-of-flight mass analyzer (LTOF).⁶¹ A stream of water vapor with a flow rate of 20 standard cubic centimeters per minute (SCCM) is passed through a high-voltage corona discharge to generate reagent ions $(\text{H}_2\text{O})_n\text{H}_3\text{O}^+$ ($n = 0,1,2,3$), which are then introduced into the FIMR. Samples are drawn into the instrument inlet at a flow rate of 3 standard liters per minute (SLPM), with 150 SCCM entering the FIMR *via* a ~ 30 mm capillary. Within the FIMR, ion-molecule reactions occur to produce product ions. The product ions are further focused and transmitted through the BSQ (RF amplitude 275 V) and the ion lens, finally reaching the back-end LTOF for detection.

In Vocus-PTR, the FIMR is the main optimization target, as both chemical ionization and ion transmission occur here simultaneously. It consists of a resistive glass tube (10 cm long) with four rods mounted radially outside (Fig. 1), establishing a focusing RF field inside the tube to confine ions into a tight beam.⁶¹ The Vocus front and back voltages are applied to the respective ends of FIMR, forming an axial electric field that propels the ions through. In addition, the internal environment is precisely controlled at specified temperature and pressure to ensure efficient ion-molecule reactions.

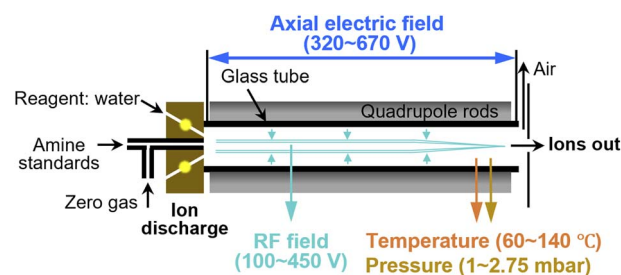
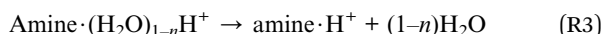
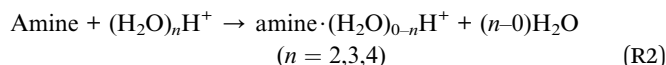
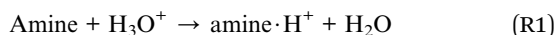


Fig. 1 The optimized parameters in focusing ion-molecular reactor (FIMR). The parameters including RF field, axial electric field, temperature, and pressure—are marked in cyan, blue, orange, and yellow, respectively.



These FIMR parameters determine the reagent ion distribution and transmission efficiency inside FIMR, thus affect the detection efficiency for amines. In previous studies, the FIMR parameters were optimized to improve the detection performance for VOCs.^{61,63–66} Higher RF amplitude achieves higher degree of ion focusing, thereby reducing wall losses during transmission. Specifically, heavier ions are more collimated towards the central axis, while lighter ions acquire higher kinetic energy.⁶³ Higher axial voltage shortens the residence time of ions within FIMR, thus reducing diffusion loss.^{63–66} Simultaneously, it results in higher collision energy between ions, which leads to a reduction in water cluster content and fragmentation of product ions.⁶⁵ Both temperature⁶⁶ and pressure^{64–66} jointly influence the distribution of reagent ions and the rate of ion-molecule reactions.

The optimization scheme is oriented towards increasing water-cluster reagent ions. It enhances amine detection in two ways: amines react with water-cluster ions *via* exothermic ligand reactions with higher reaction rates, forming more stable product ions due to excess energy transfer and hydrogen bonding, thereby enhancing the sensitivity;^{67–69} the higher proton affinity of water clusters compared with H₂O also improves selectivity for amine detection.⁶⁴ Within the FIMR, amines may undergo the following reactions ((R1)–(R3)). In Vocus-PTR, H₃O⁺ is the predominant reagent ion, making proton transfer reaction (R1) the dominant process; concurrently, water-cluster ions can also contribute to the formation of protonated or clustered product ions (R2) and (R3). The practical optimization is the process of finding the optimal trade-off between ion-molecule reaction efficiency (considering potential fragmentation of product ions) and transmission efficiency.⁶⁴



Accordingly, the parameters of the FIMR, including the RF field, axial electric field, temperature and pressure, were optimized. Generally, the ion-molecule reactor operates at its default settings of 100 °C, 2 mbar, with axial and RF amplitude voltages set to 570 V (the Vocus back voltage is fixed at 30 V) and 450 V (refers to the zero-to-peak value here and throughout), respectively. The RF field and the axial electric field were optimized first. For the RF field, it was adjusted within 100–450 V under a fixed state (axial electric field 570 V, temperature 80 °C, and pressure 2.5 mbar). For the axial electric field, the Vocus front voltage was adjusted from 350 to 700 V to achieve an axial electric field of 320–670 V under a fixed condition of Vocus back voltage 30 V, RF amplitude 450 V, temperature 60 °C and pressure 2 mbar. Temperature and pressure were co-optimized that with the RF and axial electric fields held constant, pressure was systematically varied from 1 to 2.75 mbar across a temperature gradient of 60–140 °C. The efficacy of the optimization was evaluated using 8

ppbv standard gases of MEA, PZ, AMP, DMA, and *N,N*-dimethylformamide (DMF) (see details in Section 2.2).

The reduced electric field strength (E/N) was used to characterize the distribution of reagent ions and fragmentation of ions within FIMR:⁶²

$$E/N = \frac{k_B \times \Delta V \times T}{l_{\text{FIMR}} \times p} \quad (\text{R4})$$

where k_B is the Boltzmann constant (J K⁻¹), T is the temperature (K), ΔV is the axial electric field (V), l_{FIMR} is the FIMR length (m), and p is pressure (Pa). E/N is expressed in Townsends (Td), where 1 Td = 1 × 10⁻¹⁷ V cm². Lower E/N means weaker fragmentation and more water-cluster ions. E/N analysis provided critical insights into the co-optimization process of temperature and pressure. In addition, the area ratios of the amine peaks at their corresponding unit m/z were employed to evaluate the instrument's selectivity for amine detection.

2.2 Calibration and qualification

Amine standard gases were used to evaluate the efficacy of the optimization. For MEA and DMA, standard gases were generated *via* permeation tubes (VICI Inc., USA) with certified rates of 118.59 ng min⁻¹ and 50 ng min⁻¹, respectively. The tubes were installed within a U-shaped glass tube (outer diameter: 1.8 cm; length: 28.4 cm), itself submerged in a water bath held at the recommended permeation temperatures (80 °C for MEA, 40 °C for DMA). A high-purity nitrogen stream (99.999%; 100 SCCM) acted as the carrier gas for the emitted vapors, followed by dilution with zero gas flowing at 2–8 SLPM. Generation and calibration of DMF, PZ and AMP utilized certified gas cylinders (Beijing Yongchao Xinye Technology Co., Ltd, 1 ppm, 8 MPa). Amine standards were delivered to Vocus-PTR at 4–24 SCCM and diluted with 3–8 SLPM zero gas. The product ion amine·H⁺ with the highest signal intensity was used to define its detection sensitivity. The limits of detection (LODs, 1 min) of amines were determined from zero-gas background measurement, calculated as three times the standard deviation of the background divided by the obtained sensitivity.

Several typical VOCs, including C₃H₃N, C₅H₈, C₆H₆, C₇H₈, C₈H₁₀, C₉H₁₂, and C₁₀H₁₆, were also calibrated using a certified VOC gas mixture (Beijing Yongchao Xinye Technology Co., Ltd, 1 ppm, 8 MPa) for comparison with amines. Among them, the sensitivities of C₅H₉⁺, C₈H₁₁⁺, C₉H₁₃⁺ and C₁₀H₁₇⁺ were corrected for fragmentation and cluster formation (Text S1).

For other amines or amides with no authentic standards, the sensitivities were determined through their direct linear correlation with their PTR rate constants (k_{PTR}), with corrections applied for the calculated transmission efficiency (Text S2). Details on these methodologies are also available in our previous study.⁷⁰

2.3 Field measurements

The optimized Vocus-PTR was deployed for measuring atmospheric amines from July 14th to 22nd, 2024, at an urban site in Beijing, China. Measurements were carried out on the top of a fourth-floor tower building at Tsinghua University (40°0'N, 116°20'E), with inlet positioned approximately 20 meters above



ground level. The site represents a typical residential urban environment without major traffic or industrial sources in the immediate vicinity (Fig. S1). Further details of this site can be found in our previous study.⁷¹

During the measurement, the Vocus-PTR was operated under the optimized parameters, which were set as follows: RF amplitude at 450 V, axial electric field at 570 V, temperature at 80 °C, and pressure at 2.5 mbar. A detailed description of the optimization procedure and corresponding results is presented in Section 3.1. Mass spectra were recorded at 5 second intervals across the m/z range of 11–397, achieving a mass resolution of ~ 9000 at m/z 250. Ambient air was drawn *via* a heated (50 ± 5 °C) tetrafluoroethylene (PTFE) tube (2.3 m long, 1/4-inch OD). To avoid orifice and capillary blockage, a Teflon filter was installed upstream and replaced weekly. Daily 20 minutes calibration sequences were executed, comprising 5 minutes of zero-gas background measurement and 15 minutes of rapid calibration with the certified VOC mixture, to clear residuals and verify instrument stability. On December 12th, 2024, two sequential 30-minute atmospheric measurement campaigns were performed using the pre-optimization and optimized FIMR parameters, respectively, to quantify the performance improvements attained *via* parameter optimization. The ambient mass spectra were averaged over 1 min and processed *via* Tofware v3.2.3 (Tofwerk AG & Aerodyne Research Inc.) under Igor Pro 8 (WaveMetrics, OR, USA) for mass calibration, baseline correction, and high-resolution peak fitting. Details of data processing are available in our previous studies.⁷⁰

3 Results and discussion

3.1 Performance of optimized Vocus-PTR and its optimization effects

The optimized Vocus-PTR showed good performance for both amine and VOC detection in laboratory calibration (Fig. 2). The sensitivities of amines, including DMA, MEA, PZ and AMP, are

6291, 4290, 3334, and 4488 cps per ppbv, respectively, which are comparable to those of VOCs (1076–8788 cps per ppbv). The corresponding LODs of amines are 0.55, 0.16, 0.22, and 0.16 pptv, which are lower than those of VOCs (9.34–38.79 pptv) due to their low backgrounds. Previous studies using PTR-MS or CIMS have reported LODs of 0.25–36 pptv for C₂-amines (Table S1).^{46,47,49,50,53–57,59} The LOD of C₂-amines measured in this work falls in the mid-to-upper level of this range, thus verifying the effectiveness of our optimized system for trace-level amine detection.

The optimal operating parameters in FIMR of the Vocus-PTR for trace-level amine detection were determined by investigating the effects of RF amplitude, axial electric field, and FIMR temperature and pressure on amine signal responses. With the increase of RF field and axial electric field, the instrument's response for amines both showed a pattern of first increasing and then decreasing (Fig. 3). For the RF amplitude, the signals of amines increased within most of the regulation range (300–450 V). The signals of reagent ions also increased with the rise of RF amplitude (Fig. S2a). This is because higher degree of central focusing reduced transmission loss.⁶¹ However, when the RF amplitude exceeded 450 V, the signals of amines began to decline, particularly for AMP, which may be due to its high mass-charge ratio and the higher degree of axis deflection. Charge repulsion effect under high charge density counteracted the focusing effect, while other amine ions with lighter weight gained more kinetic energy, inclining to form the target protonated product ions.^{61,63}

For the axial electric field, at voltages <570 V, the amine signals increased as higher axial voltage shortened ion residence time and reduced transmission loss in FIMR.^{63,64} However, as the axial electric field continued to increase (570–670 V), the trend turned downward. At high field strength, the average collision energy of ions increased and fragmentation of amine product ions intensified, leading to a decreased

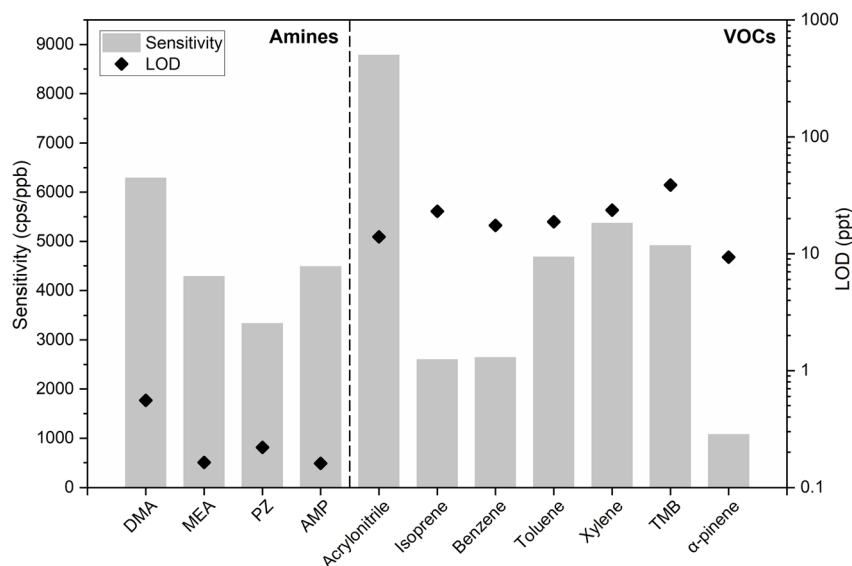


Fig. 2 Calibrated sensitivities and LODs of amines and VOCs measured by the optimized Vocus-PTR. The dotted line separates amines (left) and VOCs (right). Sensitivities are displayed as gray bars, and LODs are represented by black diamond scatters.



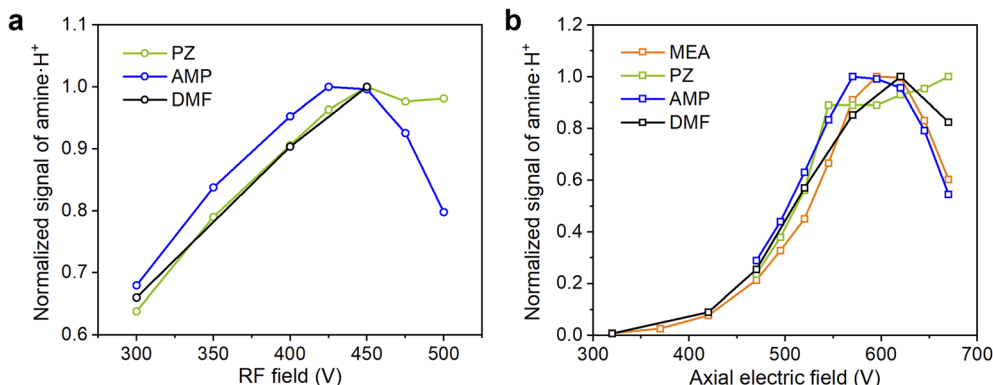


Fig. 3 Dependence of normalized amine signals on FIMR electric field parameters. (a) RF field; (b) axial electric field. Signal variations of MEA, PZ, AMP, and DMF were shown in orange, green, blue, and black, respectively.

response.^{62,65} The dependence of reagent ion signals on the axial electric field (Fig. S2b) also shows the consistent pattern. At axial electric field below 570 V, the enhancements in reagent ion signals were primarily governed by reduced ion transmission loss. When the field strength exceeded this threshold, however, the fragmentation effect intensified, as evidenced by the significantly decreased abundance of clustered reagent ions (Fig. S2b), resulting in diminished reagent ion signals. The concurrent substantial decrease in abundance of reagent ions was an additional factor contributing to the decreased amine signals. Thus, a RF amplitude of 450 V and an axial electric field of 570–620 V were selected as the optimal sets.

The FIMR temperature and pressure have a synergistic regulatory effect on amine signals by modulating the E/N value

and thus ion-molecule reaction efficiency, with amine signal variations showing an inverse trend to E/N value change (Fig. 4). Amine signals increased with rising FIMR pressure (1–2.75 mbar), consistent with the observed decrease in E/N , which was mainly attributed to elevated abundance of clustered reagent ions and reduced fragmentation of amine product ions.^{62,63,65,66} In contrast, increasing the FIMR temperature generally decreased the instrument signals for MEA and AMP, aligning with the increase in E/N . This decline was influenced by reduced clustered reagent ion abundance and enhanced fragmentation.^{62,66} However, the MEA signal increased with temperature in the range of 60–120 °C, while the PZ signal was positively correlated with temperature across the entire tested range (60–140 °C). This phenomenon may be explained by the collision-

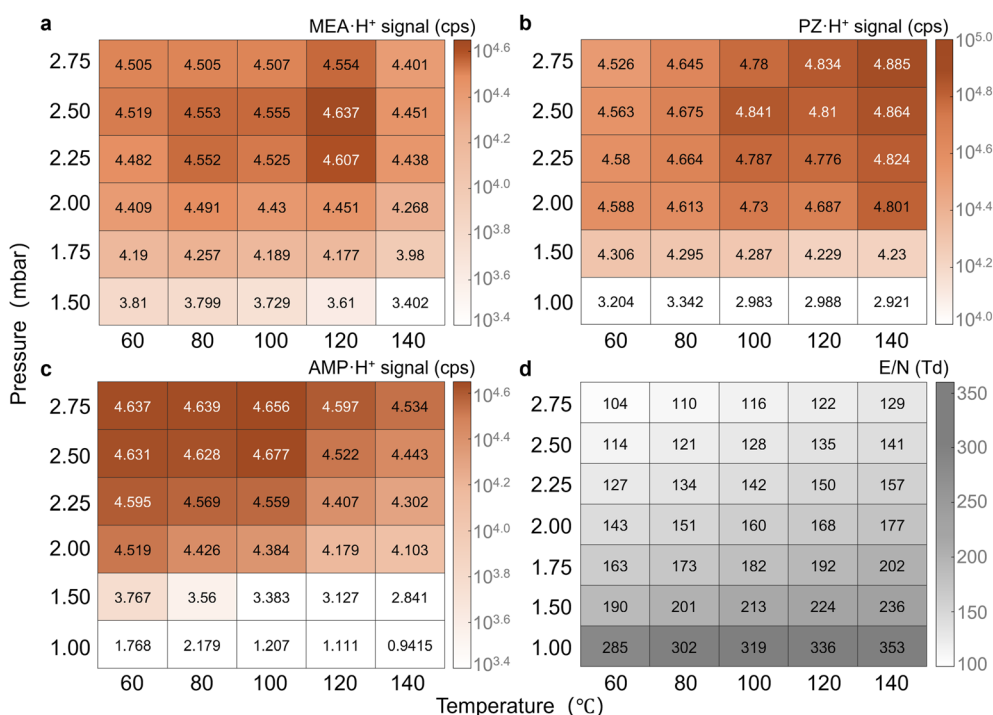


Fig. 4 Dependence of amine signals and E/N on FIMR temperature and pressure. (a) MEA; (b) PZ; (c) AMP; (d) E/N .



controlled ion-molecule reaction process in the FIMR.⁶¹ Higher temperature promotes the generation rates of amine product ions, and the ionization reactions of MEA and PZ likely possess higher activation energies, with their greater positive temperature effects compensating for the adverse influence of elevated E/N . Considering the combined trends of amine signal variations and the E/N , the temperature and pressure in FIMR were optimized to 80–100 °C and 2.5–2.75 mbar, respectively.

The abundance of water-cluster reagent ions in the FIMR increased significantly after optimization, thus improving the detection efficiency for amines. Under the optimized FIMR parameters (E/N : 107–117 Td), the content of water-cluster reagent ions in the FIMR was elevated compared with that under the default parameters (E/N : ~147 Td).⁶² As water-cluster reagent ions increased, the amine·(H₂O)H⁺/amine·H⁺ signal ratio (MEA, PZ, AMP) all showed an increasing trend (Fig. 5), indicating that elevated water-cluster reagent ions effectively promoted the formation of clustered products of amines. Given that the increase in water-cluster reagent ions was accompanied by a rise in H₃O⁺ concentration, the more distinct growth of clustered product ions with increasing water-cluster reagent ions, compared with H₃O⁺, further demonstrates their more direct role in facilitating the formation of these clustered products. Notably, although the increase in water-cluster reagent ions was the predominant driver of amine·(H₂O)H⁺ formation, clustered products might have undergone

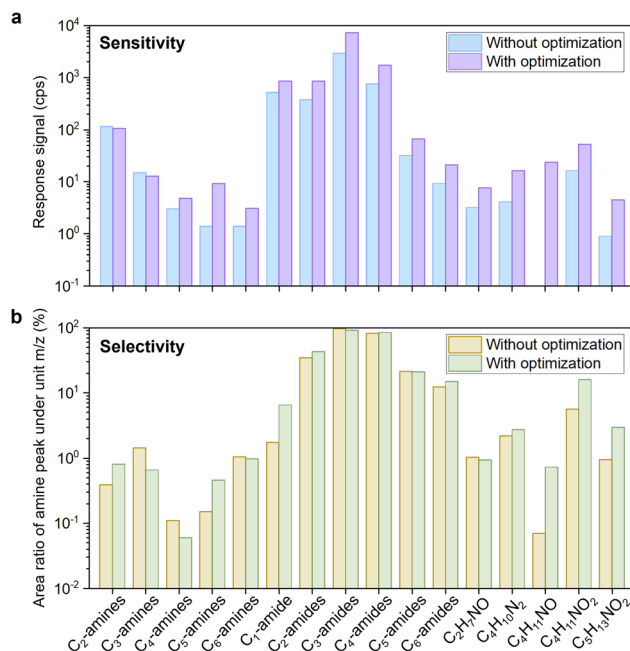


Fig. 6 Optimization effects on amine detection by Vocus-PTR in real atmosphere. (a) Measurement sensitivity for atmospheric amines. With and without optimization are represented in blue and purple, respectively. (b) Measurement selectivity for atmospheric amines. With and without optimization are represented in yellow and green, respectively.

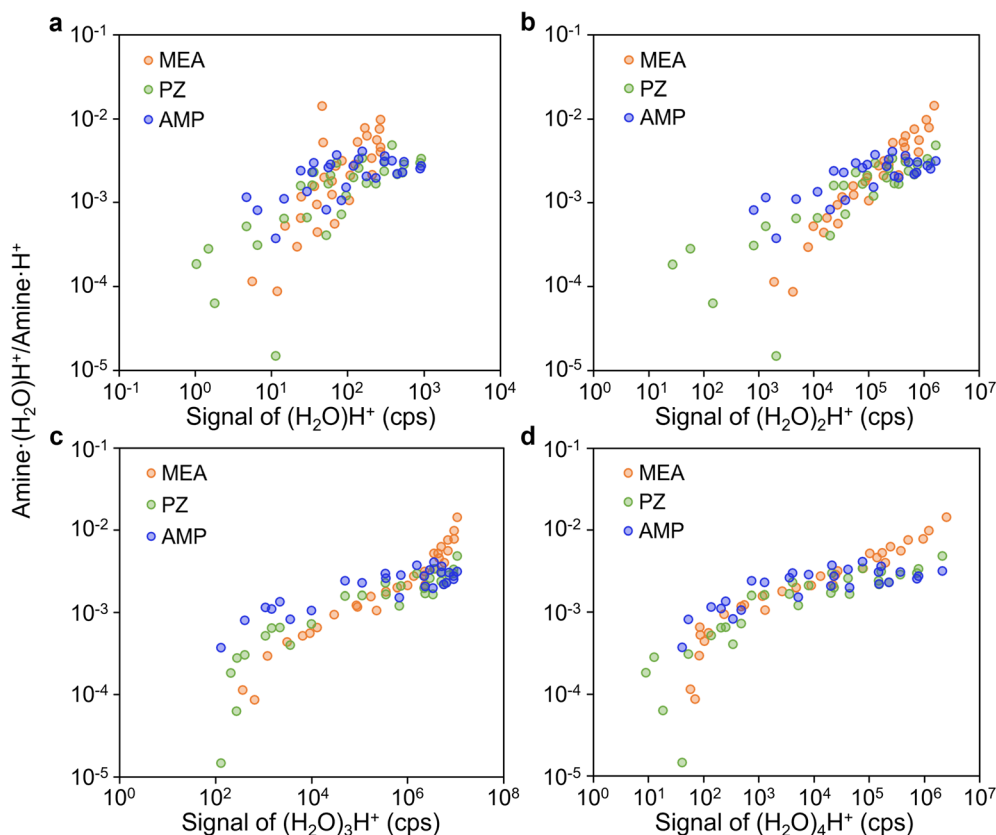


Fig. 5 Variation of amine·(H₂O)H⁺/amine·H⁺ with H₃O⁺ (a) and water-cluster reagent ions (b–d) in the FIMR.



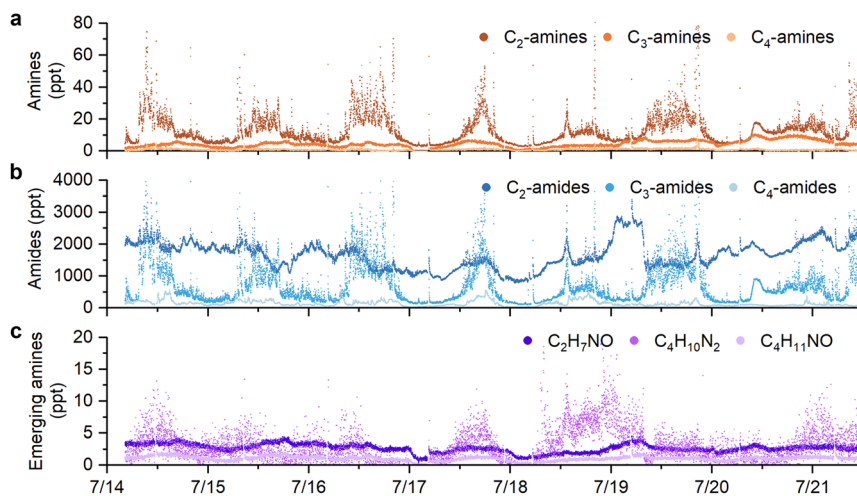


Fig. 7 Time series of typical atmospheric (a) alkylamines, (b) amides and (c) emerging amines in urban Beijing during measurement period in 2024.

dehydration during downstream transmission, finally contributing to amine·H⁺ signal.

3.2 Application in atmospheric amine measurement

C₂₋₆-amines, C₁₋₆-amides and emerging amines including C₂H₇NO, C₄H₁₀N₂, C₄H₁₁NO, C₄H₁₁NO₂ and C₅H₁₃NO₂ were observed and identified in the urban atmosphere of Beijing using the optimized Vocus-PTR (Fig. S3, 6, 7 and S4). The optimization improved the sensitivity and selectivity for these amines in real atmosphere (Fig. 6, further details are provided in Table S2). The optimized Vocus-PTR exhibited enhanced sensitivity toward various alkylamines, amides, and emerging amines with potential carbon capture relevance, with signal intensities increasing by 1.6–6.6 times. The signal of C₄H₁₁NO showed the most pronounced increase, as it was nearly undetectable prior to the optimization. Moreover, the optimized Vocus-PTR demonstrated improved selectivity for more than half of the detected amines, particularly for emerging amines, C₂-amines, C₅-amines, and the C₁-amide, whose peak areas accounted for small fractions at corresponding unit *m/z*. The improvement in selectivity further enhances the capability of the Vocus-PTR to discriminate low-concentration amines in the complex atmospheric environments. Additionally, for atmospheric VOCs (the typical species in the VOC cylinder), the response of C_xH_y showed little change or a slight decrease after optimization, while that of some C_xH_yO_z compounds increased.

During the measurement period, the average mixing ratios of the observed amines were 13.06 ± 10.47 , 4.39 ± 2.13 , 0.81 ± 0.68 , 0.05 ± 0.10 , and 0.02 ± 0.03 pptv for C₂₋₆-alkylamines; 546.3 ± 152.4 , 1662.9 ± 435.1 , 713.3 ± 731.4 , 136.77 ± 89.33 , 26.96 ± 9.81 , and 3.32 ± 1.49 pptv for C₁₋₆-amides; and 2.65 ± 0.66 , 2.98 ± 2.80 , 1.04 ± 0.35 , 2.96 ± 2.12 , and 0.77 ± 0.35 pptv for the emerging amines. The mixing ratios of alkylamines are similar to those reported for C₂-amines in Wangdu, Hebei (14.6 ± 14.9 pptv)⁴⁹ and Nanjing, Jiangsu ($0.1\text{--}29.9$ pptv),⁵⁴ yet higher than the C₂₋₃-amines concentrations measured in Beijing six

years ago⁵³ and lower than the C₂₋₆-amines concentrations measured in Shanghai.⁵⁵ The mixing ratios of both alkylamines and amides (except for C₁-amide) exhibited a decreasing trend with increasing carbon number, with C₂-amines and C₂-amides being the dominant species, in contrast to a previous result that indicated C₃-amides as predominant in Shanghai.⁵⁵ Among the emerging amines, PZ was the most abundant during the measurement period. Moreover, the mixing ratios of amides were significantly higher than those of alkylamines with the same carbon number. Comparatively, the mixing ratios of emerging amines were lower likely due to their limited sources and emissions, which may include carbon capture facilities, consumer products, *etc.*

The diurnal variations of amines were observed for these alkylamines, amides and emerging amines in urban Beijing (Fig. S5). For C₂₋₄-amines, they all exhibited a diurnal variation pattern with higher mixing ratios at night and lower levels during the daytime, consistent with previous observations in Wangdu, Hebei⁴⁹ and Beijing,⁵³ which was attributed to strong photochemical loss during the daytime. In addition, an increase in C₂-amines mixing ratios was observed around 8–9 a.m., likely influenced by traffic emissions.⁴⁹ Similar to the observation in Shanghai,⁵⁵ C₂-amide showed no distinct diurnal variation, except for a weak midday peak that may result from secondary formation. In contrast, C₃-amides and C₄-amides had higher nighttime and lower daytime mixing ratios, suggesting substantial daytime loss. As for emerging amines in the atmosphere, they exhibited no obvious diurnal pattern, which requires further investigation into their emission sources and atmospheric transformation processes.

4 Conclusions and implications

In this study, the ion-molecule reaction condition of the Vocus-PTR was optimized to enhance its detection efficiency for amines, achieving good performance for both atmospheric amines (sensitivities: 3334–6291 cps per ppbv) and VOCs



(sensitivities: 1076–8788 cps per ppbv). The RF field, axial electric field, temperature, and pressure were found to influence the detection sensitivity by affecting both the ion-molecule reaction efficiency and ion transmission efficiency within the FIMR. The observed shift in E/N (from ~ 147 to 107–117 Td) indicates that the optimization increased the abundance of water-cluster reagent ions in the FIMR, which in turn enhanced the sensitivity and selectivity for amine detection. The optimized Vocus-PTR was deployed for online measurement of atmospheric amines in urban Beijing, and C_{2-6} -amines, C_{1-6} -amides, as well as five emerging amines with potential carbon capture relevance (C_2H_7NO , $C_4H_{10}N_2$, $C_4H_{11}NO$, $C_4H_{11}NO_2$ and $C_5H_{13}NO_2$) were identified and quantified. The abundances and diurnal variations of alkylamines and alkylamides are comparable with previous studies, while demonstrating good detection capability for trace-level emerging amines.

While we have achieved improvements in the sensitivity and selectivity of Vocus-PTR for amine analysis, the peak identification of amines still faces unresolved challenges due to the limited resolution of the mass spectrometry. Even with a resolution of 9000, the LTOF mass spectrometry cannot effectively resolve well-defined, independent peaks for the majority of amines with interferences of other organic molecules. Improving mass spectrometric resolution, for instance implementing CI-Orbitrap,^{72,73} will certainly help for peak identification.

In addition, long-term observations of atmospheric amines are needed, as the scarcity of such data limits the understanding of their temporal variabilities, emission sources, and fates in the atmosphere. The optimized Vocus-PTR instrument developed in this study enables the simultaneous measurement of reactive nitrogen-containing species such as amines and their oxidation products, along with VOCs, providing an analytical foundation for future investigations of the potential interactions between them. The combination of the above instrumental advances and subsequent long-term observations will further promote a better understanding of the behavior and evolution of amines in the atmosphere.

Author contributions

Conceptualization: JJ, ZA and YZ. Data collection and analysis: YZ, ZA, JJ. Writing – original draft: YZ and ZA. Discussions, writing – review and editing: JJ, ZA, YZ, YL, RY, DL, DW, XZ, JZ, HH, JZ, KH, DRW.

Conflicts of interest

The authors declare no conflicts of interest.

Data availability

Data are available upon request from the corresponding authors.

Supplementary information (SI): the map of the measurement site (Fig. S1); dependence of normalized reagent ion signals on FIMR electric field parameters (Fig. S2); mass spectra

of identified atmospheric amines in urban Beijing in 2024 (Fig. S3); time series of emerging amines ($C_4H_{11}NO_2$ and $C_5H_{13}NO_2$) in urban Beijing during measurement period (Fig. S4); median diurnal variations of typical alkylamines, amides, and emerging amines in urban Beijing (Fig. S5). Sensitivity and LOD of instruments for C_2 -amines measurement (Table S1); improvement of atmospheric amine signal intensities (Table S2). Method for fragment and water cluster correction in Vocus-PTR (Text S1); the relationship between k_{PTR} and sensitivity, as well as the transmission efficiency in Vocus-PTR (Text S2). See DOI: <https://doi.org/10.1039/d6ea00023a>.

Acknowledgements

Financial support from National Natural Science Foundation of China (22188102, 22327806, and 22206097) and Beijing Municipal Sci-Tech Project on Ecology and Environment (BJST20250203Q) are acknowledged.

References

- M. F. Cai, B. L. Liang, Q. B. Sun, L. Liu, B. Yuan, M. Shao, S. Huang, Y. W. Peng, Z. L. Wang, H. B. Tan, *et al.*, The important roles of surface tension and growth rate in the contribution of new particle formation (NPF) to cloud condensation nuclei (CCN) number concentration: evidence from field measurements in southern China, *Atmos. Chem. Phys.*, 2021, **21**(11), 8575–8592, DOI: [10.5194/acp-21-8575-2021](https://doi.org/10.5194/acp-21-8575-2021).
- L. Yao, O. Garmash, F. Bianchi, J. Zheng, C. Yan, J. Kontkanen, H. Junninen, S. B. Mazon, M. Ehn, P. Paasonen, *et al.*, Atmospheric new particle formation from sulfuric acid and amines in a Chinese megacity, *Science*, 2018, **361**(6399), 278, DOI: [10.1126/science.aao4839](https://doi.org/10.1126/science.aao4839).
- V. Perraud, K. Roundtree, P. M. Morris, J. N. Smith and B. J. Finlayson-Pitts, Implications for new particle formation in air of the use of monoethanolamine in carbon capture and storage, *Phys. Chem. Chem. Phys.*, 2024, **26**(11), 9005–9020, DOI: [10.1039/d4cp00316k](https://doi.org/10.1039/d4cp00316k).
- S. K. W. Fomete, J. S. Johnson, N. Myllys and C. N. Jen, Experimental and Theoretical Study on the Enhancement of Alkanolamines on Sulfuric Acid Nucleation, *J. Phys. Chem. A*, 2022, **126**(25), 4057–4067, DOI: [10.1021/acs.jpca.2c01672](https://doi.org/10.1021/acs.jpca.2c01672).
- F. F. Ma, H. B. Xie, J. Elm, J. W. Shen, J. W. Chen and H. Vehkamäki, Piperazine Enhancing Sulfuric Acid-Based New Particle Formation: Implications for the Atmospheric Fate of Piperazine, *Environ. Sci. Technol.*, 2019, **53**(15), 8785–8795, DOI: [10.1021/acs.est.9b02117](https://doi.org/10.1021/acs.est.9b02117).
- C. J. Nielsen, H. Herrmann and C. Weller, Atmospheric chemistry and environmental impact of the use of amines in carbon capture and storage (CCS), *Chem. Soc. Rev.*, 2012, **41**(19), 6684–6704, DOI: [10.1039/c2cs35059a](https://doi.org/10.1039/c2cs35059a).
- M. Karl, C. Dye, N. Schmidbauer, A. Wisthaler, T. Mikoviny, B. D'Anna, M. Müller, E. Borrás, E. Clemente, A. Muñoz, *et al.*, Study of OH-initiated degradation of 2-



- aminoethanol, *Atmos. Chem. Phys.*, 2012, **12**(4), 1881–1901, DOI: [10.5194/acp-12-1881-2012](https://doi.org/10.5194/acp-12-1881-2012).
- 8 S. White, D. Angove, M. Azzi, A. Tibbett, I. Campbell and M. Patterson, An experimental investigation into the atmospheric degradation of piperazine, *Atmos. Environ.*, 2015, **108**, 133–139, DOI: [10.1016/j.atmosenv.2015.02.063](https://doi.org/10.1016/j.atmosenv.2015.02.063).
- 9 J. C. Beard and T. M. Swager, An Organic Chemist's Guide to N-Nitrosamines: Their Structure, Reactivity, and Role as Contaminants, *J. Org. Chem.*, 2021, **86**(3), 2037–2057, DOI: [10.1021/acs.joc.0c02774](https://doi.org/10.1021/acs.joc.0c02774).
- 10 H. B. Xie, F. F. Ma, Y. F. Wang, N. He, Q. Yu and J. W. Chen, Quantum Chemical Study on .Cl-Initiated Atmospheric Degradation of Monoethanolamine, *Environ. Sci. Technol.*, 2015, **49**(22), 13246–13255, DOI: [10.1021/acs.est.5b03324](https://doi.org/10.1021/acs.est.5b03324).
- 11 C. J. Nielsen, B. D'Anna, C. Dye, M. Graus, M. Karl, S. King, M. M. Maguto, M. Müller, N. Schmidbauer and Y. Stenstrom, *et al.*, Atmospheric chemistry of 2-aminoethanol (MEA), in *10th International Conference on Greenhouse Gas Control Technologies*, Amsterdam, Netherlands, 2011, vol. 4, pp 2245–2252, DOI: [10.1016/j.egypro.2011.02.113](https://doi.org/10.1016/j.egypro.2011.02.113).
- 12 N. Borduas, J. P. D. Abbatt and J. G. Murphy, Gas Phase Oxidation of Monoethanolamine (MEA) with OH Radical and Ozone: Kinetics, Products, and Particles, *Environ. Sci. Technol.*, 2013, **47**(12), 6377–6383, DOI: [10.1021/es401282j](https://doi.org/10.1021/es401282j).
- 13 V. M. Kerminen, X. M. Chen, V. Vakkari, T. Petäjä, M. Kulmala and F. Bianchi, Atmospheric new particle formation and growth: review of field observations, *Environ. Res. Lett.*, 2018, **13**(10), 103003, DOI: [10.1088/1748-9326/aadf3c](https://doi.org/10.1088/1748-9326/aadf3c).
- 14 P. Ge, G. Luo, W. Huang, H. B. Xie, J. W. Chen and Y. Luo, Theoretical study of the hydration effects on alkylamine and alkanolamine clusters and the atmospheric implication, *Chemosphere*, 2020, **243**, 125323, DOI: [10.1016/j.chemosphere.2019.125323](https://doi.org/10.1016/j.chemosphere.2019.125323).
- 15 K. F. Chen, K. Zhang and C. Qiu, Potential enhancement in atmospheric new particle formation by amine-assisted nitric acid condensation at room temperature, *Atmos. Environ.*, 2022, **287**, 119252, DOI: [10.1016/j.atmosenv.2022.119252](https://doi.org/10.1016/j.atmosenv.2022.119252).
- 16 H. B. Xie, J. Elm, R. Halonen, N. Mylly, T. Kurtén, M. Kulmala and H. Vehkamäki, Atmospheric Fate of Monoethanolamine: Enhancing New Particle Formation of Sulfuric Acid as an Important Removal Process, *Environ. Sci. Technol.*, 2017, **51**(15), 8422–8431, DOI: [10.1021/acs.est.7b02294](https://doi.org/10.1021/acs.est.7b02294).
- 17 X. L. Ge, A. S. Wexler and S. L. Clegg, Atmospheric amines - Part I. A review, *Atmos. Environ.*, 2011, **45**(3), 524–546, DOI: [10.1016/j.atmosenv.2010.10.012](https://doi.org/10.1016/j.atmosenv.2010.10.012).
- 18 IEA, *CCUS in Clean Energy Transitions*, International Energy Agency, Paris, 2020, <https://www.iea.org/reports/ccus-in-clean-energy-transitions>, Licence: CC BY 4.0.
- 19 IEA, *CCUS Projects Database*, International Energy Agency, Paris, <https://www.iea.org/data-and-statistics/data-product/ccus-projects-database>, License: CC BY 4.0.
- 20 X. Zhang, X. Yang and X. Lu, *et al.*, *China Carbon Capture, Utilization, and Storage (CCUS) Annual Report 2023; China 21st Century Agenda Management Center*, Global CCS Institute, Tsinghua University, 2023.
- 21 Z. W. Liang, K. Y. Fu, R. Idem and P. Tontiwachwuthikul, Review on current advances, future challenges and consideration issues for post-combustion CO₂ capture using amine-based absorbents, *Chin. J. Chem. Eng.*, 2016, **24**(2), 278–288, DOI: [10.1016/j.cjche.2015.06.013](https://doi.org/10.1016/j.cjche.2015.06.013).
- 22 R. Neerup, V. E. Rasmussen, S. H. B. Vinjarapu, A. H. Larsen, M. Shi, C. Andersen, K. Fuglsang, L. K. Gram, J. Nedenskov, J. Kappel, *et al.*, Solvent degradation and emissions from a CO₂ capture pilot at a waste-to-energy plant, *J. Environ. Chem. Eng.*, 2023, **11**(6), 111411, DOI: [10.1016/j.jece.2023.111411](https://doi.org/10.1016/j.jece.2023.111411).
- 23 P. Khakharia, H. M. Kvamsdal, E. F. da Silva, T. J. H. Vlught and E. Goetheer, Field study of a Brownian Demister Unit to reduce aerosol based emission from a Post Combustion CO₂ Capture plant, *Int. J. Greenh. Gas Control*, 2014, **28**, 57–64, DOI: [10.1016/j.ijggc.2014.06.022](https://doi.org/10.1016/j.ijggc.2014.06.022).
- 24 E. F. da Silva, H. Kolderup, E. Goetheer, K. W. Hjarbo, A. Huizinga, P. Khakharia, I. Tuinman, T. Mejdell, K. Zahlens and K. Vernstad, *et al.*, Emission studies from a CO₂ capture pilot plant, in *International Conference on Greenhouse Gas Technologies (GHGT)*, Kyoto, Japan, 2013, vol. 37, pp 778–783, DOI: [10.1016/j.egypro.2013.05.167](https://doi.org/10.1016/j.egypro.2013.05.167).
- 25 J. G. Thompson, M. Combs, K. Abad, S. Bhatnagar, J. Pelgen, M. Beaudry, G. Rochelle, S. Hume, D. Link, J. Figueroa, *et al.*, Pilot testing of a heat integrated 0.7 MWe CO₂ capture system with two-stage air-stripping: Emission, *Int. J. Greenh. Gas Control*, 2017, **64**, 267–275, DOI: [10.1016/j.ijggc.2017.08.003](https://doi.org/10.1016/j.ijggc.2017.08.003).
- 26 P. Moser, G. Wiechers, S. Schmidt, J. Monteiro, E. Goetheer, C. Charalambous, A. Saleh, M. van der Spek and S. Garcia, ALIGN-CCUS: Results of the 18-month test with aqueous AMP/PZ solvent at the pilot plant at Niederaussem-solvent management, emissions and dynamic behavior, *Int. J. Greenh. Gas Control*, 2021, **109**, 103381, DOI: [10.1016/j.ijggc.2021.103381](https://doi.org/10.1016/j.ijggc.2021.103381).
- 27 P. Khakharia, A. Huizinga, C. J. Lopez, C. S. Sanchez, F. D. Mercader, T. J. H. Vlught and E. Goetheer, Acid Wash Scrubbing as a Countermeasure for Ammonia Emissions from a Postcombustion CO₂ Capture Plant, *Ind. Eng. Chem. Res.*, 2014, **53**(33), 13195–13204, DOI: [10.1021/ie502045c](https://doi.org/10.1021/ie502045c).
- 28 P. Moser, G. Wiechers, S. Schmidt, J. Monteiro, C. Charalambous, S. Garcia and E. S. Fernandez, Results of the 18-month test with MEA at the post-combustion capture pilot plant at Niederaussem - new impetus to solvent management, emissions and dynamic behaviour, *Int. J. Greenh. Gas Control*, 2020, **95**, 102945, DOI: [10.1016/j.ijggc.2019.102945](https://doi.org/10.1016/j.ijggc.2019.102945).
- 29 G. T. Rochelle, K. Akinpelumi, T. Y. Gao, C. T. Liu, A. S. Babu and Y. Y. Wu, Pilot plant results with the piperazine advanced stripper at NGCC conditions, *Int. J. Greenh. Gas Control*, 2022, **113**, 103551, DOI: [10.1016/j.ijggc.2021.103551](https://doi.org/10.1016/j.ijggc.2021.103551).
- 30 J. N. Knudsen, O. M. Bade, I. Askestad, O. Gorset and T. Mejdell, Pilot plant demonstration of CO₂ capture from cement plant with advanced amine technology, in *12th International Conference on Greenhouse Gas Control*



- Technologies (GHGT)*, Austin, TX, 2014, vol. 63, pp 6464–6475, DOI: [10.1016/j.egypro.2014.11.682](https://doi.org/10.1016/j.egypro.2014.11.682).
- 31 L. Zhu, G. W. Schade and C. J. Nielsen, Real-Time Monitoring of Emissions from Monoethanolamine-Based Industrial Scale Carbon Capture Facilities, *Environ. Sci. Technol.*, 2013, **47**(24), 14306–14314, DOI: [10.1021/es4035045](https://doi.org/10.1021/es4035045).
- 32 A. K. Morken, S. Pedersen, E. R. Kleppe, A. Wisthaler, K. Vernstad, O. Ullestad, N. E. Flo, L. Faramarzi and E. S. Hamborg, Degradation and Emission Results of Amine Plant Operations from MEA Testing at the CO₂ Technology Centre Mongstad, in *13th International Conference on Greenhouse Gas Control Technologies (GHGT)*, Lausanne, Switzerland, 2017, vol. 114, pp 1245–1262, DOI: [10.1016/j.egypro.2017.03.1379](https://doi.org/10.1016/j.egypro.2017.03.1379).
- 33 M. Akyüz, Simultaneous determination of aliphatic and aromatic amines in indoor and outdoor air samples by gas chromatography-mass spectrometry, *Talanta*, 2007, **71**(1), 486–492, DOI: [10.1016/j.talanta.2006.10.028](https://doi.org/10.1016/j.talanta.2006.10.028).
- 34 M. Akyüz, Simultaneous determination of aliphatic and aromatic amines in ambient air and airborne particulate matters by gas chromatography-mass spectrometry, *Atmos. Environ.*, 2008, **42**(16), 3809–3819, DOI: [10.1016/j.atmosenv.2007.12.057](https://doi.org/10.1016/j.atmosenv.2007.12.057).
- 35 M. L. Dawson, V. Perraud, A. Gomez, K. D. Arquero, M. J. Ezell and B. J. Finlayson-Pitts, Measurement of gas-phase ammonia and amines in air by collection onto an ion exchange resin and analysis by ion chromatography, *Atmos. Meas. Tech.*, 2014, **7**(8), 2733–2744, DOI: [10.5194/amt-7-2733-2014](https://doi.org/10.5194/amt-7-2733-2014).
- 36 N. Freshour, K. Carlson, Y. Melka, S. Hinz, B. Panta and D. Hanson, Quantifying amine permeation sources with acid neutralization: calibrations and amines measured in coastal and continental atmospheres, *Atmos. Meas. Tech. Discuss.*, 2014, **7**(4), 3835–3861.
- 37 H. Feng, X. Ye, Y. Liu, Z. Wang, T. Gao, A. Cheng, X. Wang and J. Chen, Simultaneous determination of nine atmospheric amines and six inorganic ions by non-suppressed ion chromatography using acetonitrile and 18-crown-6 as eluent additive, *J. Chromatogr. A*, 2020, **1624**, 461234, DOI: [10.1016/j.chroma.2020.461234](https://doi.org/10.1016/j.chroma.2020.461234).
- 38 H. Hellén, A. J. Kieloaho and H. Hakola, Gas-phase alkyl amines in urban air; comparison with a boreal forest site and importance for local atmospheric chemistry, *Atmos. Environ.*, 2014, **94**, 192–197, DOI: [10.1016/j.atmosenv.2014.05.029](https://doi.org/10.1016/j.atmosenv.2014.05.029).
- 39 M. A. Iqbal, J. E. Szulejko and K. H. Kim, Determination of methylamine, dimethylamine, and trimethylamine in air by high-performance Liquid chromatography with derivatization using 9-fluorenylmethylchloroformate, *Anal. Methods*, 2014, **6**(15), 5697–5707, DOI: [10.1039/c4ay00740a](https://doi.org/10.1039/c4ay00740a).
- 40 A. J. Kieloaho, H. Hellén, H. Hakola, H. E. Manninen, T. Nieminen, M. Kulmala and M. Pihlatie, Gas-phase alkylamines in a boreal Scots pine forest air, *Atmos. Environ.*, 2013, **80**, 369–377, DOI: [10.1016/j.atmosenv.2013.08.019](https://doi.org/10.1016/j.atmosenv.2013.08.019).
- 41 M. van Pinxteren, K. W. Fomba, D. van Pinxteren, N. Triesch, E. H. Hoffmann, C. H. L. Cree, M. F. Fitzsimons, W. von Tümpling and H. Herrmann, Aliphatic amines at the Cape Verde Atmospheric Observatory: Abundance, origins and sea-air fluxes, *Atmos. Environ.*, 2019, **203**, 183–195, DOI: [10.1016/j.atmosenv.2019.02.011](https://doi.org/10.1016/j.atmosenv.2019.02.011).
- 42 T. C. VandenBoer, M. Z. Markovic, A. Petroff, M. F. Czar, N. Borduas and J. G. Murphy, Ion chromatographic separation and quantitation of alkyl methylamines and ethylamines in atmospheric gas and particulate matter using preconcentration and suppressed conductivity detection, *J. Chromatogr. A*, 2012, **1252**, 74–83, DOI: [10.1016/j.chroma.2012.06.062](https://doi.org/10.1016/j.chroma.2012.06.062).
- 43 F. X. Liu, X. H. Bi, G. H. Zhang, X. F. Lian, Y. Z. Fu, Y. X. Yang, Q. H. Lin, F. Jiang, X. M. Wang, P. A. Peng, *et al.*, Gas-to-particle partitioning of atmospheric amines observed at a mountain site in southern China, *Atmos. Environ.*, 2018, **195**, 1–11, DOI: [10.1016/j.atmosenv.2018.09.038](https://doi.org/10.1016/j.atmosenv.2018.09.038).
- 44 I. H. Chang, C. G. Lee and D. S. Lee, Development of an automated method for simultaneous determination of low molecular weight aliphatic amines and ammonia in ambient air by diffusion scrubber coupled to ion chromatography, *Anal. Chem.*, 2003, **75**(22), 6141–6146, DOI: [10.1021/ac0347314](https://doi.org/10.1021/ac0347314).
- 45 M. van Pinxteren, K. W. Fomba, D. van Pinxteren, N. Triesch, E. H. Hoffmann, C. H. L. Cree, M. F. Fitzsimons, W. von Tümpling and H. Herrmann, Aliphatic amines at the Cape Verde Atmospheric Observatory: Abundance, origins and sea-air fluxes, *Atmos. Environ.*, 2019, **203**, 183–195, DOI: [10.1016/j.atmosenv.2019.02.011](https://doi.org/10.1016/j.atmosenv.2019.02.011).
- 46 D. R. Hanson, P. H. McMurry, J. Jiang, D. Tanner and L. G. Huey, Ambient Pressure Proton Transfer Mass Spectrometry: Detection of Amines and Ammonia, *Environ. Sci. Technol.*, 2011, **45**(20), 8881–8888, DOI: [10.1021/es201819a](https://doi.org/10.1021/es201819a).
- 47 K. Sellegri, B. Umann, M. Hanke and F. Arnold, Deployment of a ground-based CIMS apparatus for the detection of organic gases in the boreal forest during the QUEST campaign, *Atmos. Chem. Phys.*, 2005, **5**, 357–372, DOI: [10.5194/acp-5-357-2005](https://doi.org/10.5194/acp-5-357-2005).
- 48 N. Freshour, K. Carlson, Y. Melka, S. Hinz, B. Panta and D. Hanson, Quantifying amine permeation sources with acid neutralization: calibrations and amines measured in coastal and continental atmospheres, *Atmos. Meas. Tech. Discuss.*, 2014, **7**(4), 3835–3861.
- 49 Y. W. Wang, G. Yang, Y. Q. Lu, Y. L. Liu, J. M. Chen and L. Wang, Detection of gaseous dimethylamine using Vocus proton-transfer-reaction time-of-flight mass spectrometry, *Atmos. Environ.*, 2020, **243**, 117875, DOI: [10.1016/j.atmosenv.2020.117875](https://doi.org/10.1016/j.atmosenv.2020.117875).
- 50 Y. Chang, H. Wang, Y. Gao, S. Jing, Y. Lu, S. Lou, Y. Kuang, K. Cheng, Q. Ling, L. Zhu, *et al.*, Nonagricultural emissions dominate urban atmospheric amines as revealed by mobile measurements, *Geophys. Res. Lett.*, 2022, e2021GL097640, DOI: [10.1029/2021gl097640](https://doi.org/10.1029/2021gl097640).
- 51 Y. Chang, Y. N. Feng, L. Cheng, J. Hu, L. Zhu, W. Tan, H. Zhong, Y. Zhang, R. J. Huang and Y. Sun,



- Trimethylamine from Subtropical Forests Rival Total Farmland Emissions in China, *Environ. Sci. Technol.*, 2024, **58**(12), 5453–5460, DOI: [10.1021/acs.est.4c00622](https://doi.org/10.1021/acs.est.4c00622).
- 52 J. Pfeifer, M. Simon, M. Heinritzi, F. Piel, L. Weitz, D. Y. Wang, M. Granzin, T. Müller, S. Bräkling, J. Kirkby, *et al.*, Measurement of ammonia, amines and iodine compounds using protonated water cluster chemical ionization mass spectrometry, *Atmos. Meas. Tech.*, 2020, **13**(5), 2501–2522, DOI: [10.5194/amt-13-2501-2020](https://doi.org/10.5194/amt-13-2501-2020).
- 53 S. N. Zhu, C. Yan, J. Zheng, C. Chen, H. S. Ning, D. S. Yang, M. Wang, Y. Ma, J. L. Zhan, C. J. Hua, *et al.*, Observation and Source Apportionment of Atmospheric Alkaline Gases in Urban Beijing, *Environ. Sci. Technol.*, 2022, **56**(24), 17545–17555, DOI: [10.1021/acs.est.2c03584](https://doi.org/10.1021/acs.est.2c03584).
- 54 J. Zheng, Y. Ma, M. D. Chen, Q. Zhang, L. Wang, A. F. Khalizov, L. Yao, Z. Wang, X. Wang and L. X. Chen, Measurement of atmospheric amines and ammonia using the high resolution time-of-flight chemical ionization mass spectrometry, *Atmos. Environ.*, 2015, **102**, 249–259, DOI: [10.1016/j.atmosenv.2014.12.002](https://doi.org/10.1016/j.atmosenv.2014.12.002).
- 55 L. Yao, M. Y. Wang, X. K. Wang, Y. J. Liu, H. F. Chen, J. Zheng, W. Nie, A. J. Ding, F. H. Geng, D. F. Wang, *et al.*, Detection of atmospheric gaseous amines and amides by a high-resolution time-of-flight chemical ionization mass spectrometer with protonated ethanol reagent ions, *Atmos. Chem. Phys.*, 2016, **16**(22), 14527–14543, DOI: [10.5194/acp-16-14527-2016](https://doi.org/10.5194/acp-16-14527-2016).
- 56 Y. You, V. P. Kanawade, J. A. de Gouw, A. B. Guenther, S. Madronich, M. R. Sierra-Hernández, M. Lawler, J. N. Smith, S. Takahama, G. Ruggeri, *et al.*, Atmospheric amines and ammonia measured with a chemical ionization mass spectrometer (CIMS), *Atmos. Chem. Phys.*, 2014, **14**(22), 12181–12194, DOI: [10.5194/acp-14-12181-2014](https://doi.org/10.5194/acp-14-12181-2014).
- 57 L. Tiszenkel, J. H. Flynn and S. H. Lee, Measurement report: Urban ammonia and amines in Houston, Texas, *Atmos. Chem. Phys.*, 2024, **24**(19), 11351–11363, DOI: [10.5194/acp-24-11351-2024](https://doi.org/10.5194/acp-24-11351-2024).
- 58 H. Yu and S. H. Lee, Chemical ionisation mass spectrometry for the measurement of atmospheric amines, *Environ. Chem.*, 2012, **9**(3), 190–201, DOI: [10.1071/en12020](https://doi.org/10.1071/en12020).
- 59 M. Simon, M. Heinritzi, S. Herzog, M. Leiminger, F. Bianchi, A. Praplan, J. Dommen, J. Curtius and A. Kürten, Detection of dimethylamine in the low pptv range using nitrate chemical ionization atmospheric pressure interface time-of-flight (CI-API-TOF) mass spectrometry, *Atmos. Meas. Tech.*, 2016, **9**(5), 2135–2145, DOI: [10.5194/amt-9-2135-2016](https://doi.org/10.5194/amt-9-2135-2016).
- 60 T. Mikoviny, C. J. Nielsen, W. Tan, A. Wisthaler, L. Zhu, A. K. Morken and T. N. Nilsen, Ambient Measurements of Amines by PTR-QiTOF: Instrument Performance Assessment and Results from Field Measurements in the Vicinity of TCM, Mongstad, in *13th International Conference on Greenhouse Gas Control Technologies (GHGT)*, Lausanne, Switzerland, 2017, vol. 114, pp 1017–1021, DOI: [10.1016/j.egypro.2017.03.1246](https://doi.org/10.1016/j.egypro.2017.03.1246).
- 61 J. Krechmer, F. Lopez-Hilfiker, A. Koss, M. Hutterli, C. Stoermer, B. Deming, J. Kimmel, C. Warneke, R. Holzinger, J. Jayne, *et al.*, Evaluation of a New Reagent Ion Source and Focusing Ion-Molecule Reactor for Use in Proton-Transfer-Reaction Mass Spectrometry, *Anal. Chem.*, 2018, **90**(20), 12011–12018, DOI: [10.1021/acs.analchem.8b02641](https://doi.org/10.1021/acs.analchem.8b02641).
- 62 M. F. Link, M. S. Claffin, C. E. Cecelski, A. A. Akande, D. Kilgour, P. A. Heine, M. Coggon, C. E. Stockwell, A. Jensen, J. Yu, *et al.*, Product ion distributions using H₃O⁺ proton-transfer-reaction time-of-flight mass spectrometry (PTR-ToF-MS): mechanisms, transmission effects, and instrument-to-instrument variability, *Atmos. Meas. Tech.*, 2025, **18**(4), 1013–1038, DOI: [10.5194/amt-18-1013-2025](https://doi.org/10.5194/amt-18-1013-2025).
- 63 F. Li, D. D. Huang, L. Tian, B. Yuan, W. Tan, L. Zhu, P. Ye, D. Worsnop, K. I. Hoi, K. M. Mok, *et al.*, Response of protonated, adduct, and fragmented ions in Vocus proton-transfer-reaction time-of-flight mass spectrometer (PTR-ToF-MS), *Atmos. Meas. Tech.*, 2024, **17**(8), 2415–2427, DOI: [10.5194/amt-17-2415-2024](https://doi.org/10.5194/amt-17-2415-2024).
- 64 C. L. Zang and M. D. Willis, Deployment and evaluation of an NH₄⁺/H₃O⁺ reagent ion switching chemical ionization mass spectrometer for the detection of reduced and oxygenated gas-phase organic compounds, *Atmos. Meas. Tech.*, 2025, **18**(1), 17–35, DOI: [10.5194/amt-18-17-2025](https://doi.org/10.5194/amt-18-17-2025).
- 65 H. Li, T. G. Almeida, Y. Luo, J. Zhao, B. B. Palm, C. D. Daub, W. Huang, C. Mohr, J. E. Krechmer, T. Kurtén, *et al.*, Fragmentation inside proton-transfer-reaction-based mass spectrometers limits the detection of ROOR and ROOH peroxides, *Atmos. Meas. Tech.*, 2022, **15**(6), 1811–1827, DOI: [10.5194/amt-15-1811-2022](https://doi.org/10.5194/amt-15-1811-2022).
- 66 L. Xu, M. M. Coggon, C. E. Stockwell, J. B. Gilman, M. A. Robinson, M. Breitenlechner, A. Lamplugh, J. D. Crouse, P. O. Wennberg, J. A. Neuman, *et al.*, Chemical ionization mass spectrometry utilizing ammonium ions (NH₄⁺ CIMS) for measurements of organic compounds in the atmosphere, *Atmos. Meas. Tech.*, 2022, **15**(24), 7353–7373, DOI: [10.5194/amt-15-7353-2022](https://doi.org/10.5194/amt-15-7353-2022).
- 67 A. Hansel, W. Scholz, B. Mentler, L. Fischer and T. Berndt, Detection of RO₂ radicals and other products from cyclohexene ozonolysis with NH₄⁺ and acetate chemical ionization mass spectrometry, *Atmos. Environ.*, 2018, **186**, 248–255, DOI: [10.1016/j.atmosenv.2018.04.023](https://doi.org/10.1016/j.atmosenv.2018.04.023).
- 68 M. Breitenlechner, L. Fischer, M. Hainer, M. Heinritzi, J. Curtius and A. Hansel, PTR3: An Instrument for Studying the Lifecycle of Reactive Organic Carbon in the Atmosphere, *Anal. Chem.*, 2017, **89**(11), 5825–5832, DOI: [10.1021/acs.analchem.6b05110](https://doi.org/10.1021/acs.analchem.6b05110).
- 69 B. H. Lee, F. D. Lopez-Hilfiker, C. Mohr, T. Kurtén, D. R. Worsnop and J. A. Thornton, An Iodide-Adduct High-Resolution Time-of-Flight Chemical-Ionization Mass Spectrometer: Application to Atmospheric Inorganic and Organic Compounds, *Environ. Sci. Technol.*, 2014, **48**(11), 6309–6317, DOI: [10.1021/es500362a](https://doi.org/10.1021/es500362a).
- 70 Z. An, R. Yin, X. Zhao, X. Li, Y. Li, Y. Yuan, J. Guo, Y. Zhao, X. Li, D. Li, *et al.*, Molecular and seasonal characteristics of organic vapors in urban Beijing: insights from Vocus-PTR measurements, *Atmos. Chem. Phys.*, 2024, **24**(23), 13793–13810, DOI: [10.5194/acp-24-13793-2024](https://doi.org/10.5194/acp-24-13793-2024).



- 71 R. Cai and J. Jiang, A new balance formula to estimate new particle formation rate: reevaluating the effect of coagulation scavenging, *Atmos. Chem. Phys.*, 2017, 17(20), 12659–12675, DOI: [10.5194/acp-17-12659-2017](https://doi.org/10.5194/acp-17-12659-2017).
- 72 Y. Yuan, X. Chen, R. L. Cai, X. X. Li, Y. Y. Li, R. J. Yin, D. D. Li, C. Yan, Y. C. Liu, K. B. He, *et al.*, Resolving Atmospheric Oxygenated Organic Molecules in Urban Beijing Using Online Ultrahigh-Resolution Chemical Ionization Mass Spectrometry, *Environ. Sci. Technol.*, 2024, 58(40), 17777–17785, DOI: [10.1021/acs.est.4c04214](https://doi.org/10.1021/acs.est.4c04214).
- 73 Y. Q. Zhao, Z. T. Yan, Z. J. An, Y. Y. Li, R. J. Yin, D. D. Li, Y. Chen, D. B. Wang, H. B. Xie, J. Zheng, *et al.*, Emerging Amines in the Atmosphere: Occurrence and Potential Relevance to Carbon Capture, *Environ. Sci. Technol. Lett.*, 2026, 13, 532–539, DOI: [10.1021/acs.estlett.6c00083](https://doi.org/10.1021/acs.estlett.6c00083).

